

Two-Particle Microrheology of quasi-2D Viscous Systems

V. Prasad, S. A. Koehler, and Eric R. Weeks

Department of Physics, Emory University, Atlanta, GA 30322

(Dated: March 20, 2019)

We study the correlated motions of colloidal particles in a quasi-2D system (Human Serum Albumin (HSA) protein molecules at an air-water interface) for different surface viscosities η_s . We observe a transition in the behavior of the correlated motion, from 2-D interfacial dominated at high η_s to bulk fluid-dependent at low η_s . The correlated motions can be scaled onto a master curve which captures the features of this transition. This master curve also characterizes the spatial dependence of the flow field of a viscous interface in response to a force. From the flow field and the correlated particle motions, we calculate a two-particle MSD (mean square displacement) for direct comparison with rheological measurements.

PACS numbers: 83.10.Mj, 87.68.+z, 87.16.Dg

Diffusion in three dimensions has been well understood since 1905, when two authors showed that the motion of particles suspended in a fluid is related to the fluid's viscosity [1, 2]. This observation has been generalized in a technique called microrheology, which measures the thermal motion of tracer particles introduced in a viscoelastic material. From the motions of the particles, the material dependent properties such as the elastic modulus, $G'(\omega)$, and the viscous modulus, $G''(\omega)$, can be determined [3]. This has been applied to measure the viscoelasticity of bulk materials such as polymer solutions [4], biomaterials [5] and hydrogels [6]. A closely related question is the motion of tracer particles in a two-dimensional system such as lipid molecules at an air-water interface [7] or lipid rafts in cell membranes [8]. For example, in a purely viscous 2-D system, one might imagine that the diffusive properties are related to the two-dimensional viscosity, and that by following the motion of tracer particles one could determine this viscosity. However, in most cases of practical interest, a strictly two-dimensional surface is an idealization and in reality the surface is adjacent to three-dimensional fluid reservoirs. For example, recent experiments study diffusion in biological systems such as cell membranes [8, 9] which are surrounding a 3-D cell and immersed in a 3-D fluid. This coupling modifies the behavior of tracer particles and makes interpretation of the results trickier [10, 11, 12].

Furthermore, in many cases in 3D, tracers are known to modify the structure of the medium in their vicinity, leading to erroneous measurements of rheological quantities [13]. Another possibility is that pre-existing inhomogeneities such as pores in an otherwise rigid material can entrain the tracers, resulting in measurements that underestimate the bulk viscoelasticity of the material in question [5]. To overcome these difficulties, a new method known as two-particle microrheology has been established [13], which looks at the cross-correlated thermal motions of pairs of particles. The correlated motion of two beads is driven by long-wavelength modes in the system, and is therefore independent of the local environment of the tracers. While two-particle microrheology has been applied to 3-D systems [13, 14] where the

strain field decays as $1/R$, a formalism for 2-D interfacial systems coupled to viscous bulk fluids has not been experimentally determined to date. This is largely due to the non-trivial nature of the flow field created by the thermal motion of particles at an interface. An understanding of this flow field is critical towards determining the true microrheological behavior of an interface [7, 8, 9].

In this Letter, we look at the correlated motions of particles embedded at an air-water interface in the presence of human serum albumin (HSA) protein molecules. This is done as a function of particle separation R and lag times τ , for correlated motion along the line joining the centers of particles, $D_{rr}(R; \tau)$, and motion perpendicular, $D_{\perp}(R; \tau)$. The interface is purely viscous, with $D_{rr}, D_{\perp} \propto \eta_s \tau$. The averaged quantities $\langle D_{rr} \rangle = \langle D_{\perp} \rangle$ show a transition as a function of the surface viscosity η_s ; at high η_s their behavior is 2-D dominated; at intermediate η_s they show crossover behavior; and at low η_s their behavior is strongly influenced by the 3-D fluid reservoirs ($\langle D_{rr} \rangle \propto 1/R$ and $\langle D_{\perp} \rangle \propto 1/R^2$ respectively). The correlated motion of the tracer particles for different surface viscosities can be scaled onto a single master curve, which agrees with theoretical predictions [15]. Moreover, the scaled master curve is used to determine a two-particle MSD (mean square displacement) of the systems, which compares well with the one-particle MSDs, demonstrating the homogeneity of HSA at an interface.

We use aqueous solutions of HSA over a narrow range of bulk concentrations ($c = 0.03 - 0.045$ mg/ml) to obtain our interface. At these bulk concentrations, HSA molecules diffuse to the air-water interface to form a thin monolayer of size ≈ 3 nm [16], thereby creating a surface shear viscosity. The surface concentration of HSA slowly increases over time [17], and so the surface shear viscosity η_s can be varied over a wide range. The viscosity of the bulk solution is negligibly different from the viscosity of water, and is assumed to be $\eta = 1.0$ mPas for all our experiments, while the viscosity of air is considered to be negligible. Micron-sized polystyrene beads (Interfacial Dynamics Corporation, carboxyl-modified, radius $a = 0.9$ μ m) dispersed in an aqueous solution with 20% isopropyl alcohol, are spread at the interface with a syringe

needle to act as tracer particles. The particles are imaged by bright-field microscopy with a 20 \times objective, NA = 0.45, at a spatial resolution of 606 nm/pixel and a frame rate of 30 Hz. For each sample, short movies of 200 frames are recorded with a CCD camera (Integrated Design Tools, X-Stream Vision XS-3) that has 1240 \times 1024 pixel resolution, with hundreds of particles lying within the field of view.

The positions of the tracers are determined by particle tracking. From the particle positions, we also determine the vector displacements of the tracers $\mathbf{r}(t; \tau) = \mathbf{r}(t + \tau) - \mathbf{r}(t)$ where t is the absolute time and τ is the lag time. Care is taken to eliminate any global drift of the sample from these vector displacements. We can then calculate the ensemble-averaged cross-correlated particle motions [13]

$$D_{ij}(\mathbf{r}; \tau) = \langle \mathbf{r}_i^T(\mathbf{r}; \tau) \mathbf{r}_j(\mathbf{r}; \tau) [\mathbf{r} \cdot \mathbf{R}^{ij}(\mathbf{r})]_{i \neq j} \rangle \quad (1)$$

where i, j are particle indices, and represent different co-ordinates and \mathbf{R}^{ij} is the distance between particles i and j . In particular, we focus on the diagonal elements of this tensor product: D_{rr} , which measures the correlated motion along the line joining the centers of particles, and $D_{\theta\theta}$, which measures the correlated motion perpendicular to this line (the off-diagonal elements are assumed to be uncorrelated, and hence 0). In addition, we also calculate the one-particle MSD, $\langle r^2(\tau) \rangle_i$, from the self terms ($i = j$) in the above expression. In 2-D interfacial systems coupled to a bulk fluid reservoir, this one-particle MSD is related to the surface viscosity η_s by a modified Stokes-Einstein relation [10, 11, 12]

$$\langle r^2(\tau) \rangle_i = 4D_s^0 \tau \quad (2)$$

where $D_s^0 = D_s [\ln(2\eta_s/a) - \zeta_E]$ (valid in the limit $\eta_s = a^{-1}$), with $D_s = k_B T/4\eta_s$ and $\zeta_E = 0.577$ being Euler's constant. Using the measured values of $\langle r^2(\tau) \rangle_i$, we solve this equation to obtain one-particle surface viscosities, $\eta_{s,1p}$ (refer inset of Fig. 1 for example). To check the validity of these intrinsically local one-particle measurements, we also perform two-particle measurements, the formalism of which is described below.

In Fig. 1 (a), we show D_{rr} as a function of R for different lag times τ , for a sample with $\eta_{s,1p} = 340$ nPa s m. The motion of a tracer particle creates a flow field that affects the motion of other particles. This flow field decays as we move further out from the particle; hence the correlated motions decay as a function of particle separation for all lag times. From the one-particle measurements, we observe that HSA monolayers at an interface are entirely viscous at these surface concentrations, and therefore we also observe that $D_{rr} \propto R^{-1}$. This is illustrated in Fig. 1 (a) where all the D_{rr} are spaced evenly on a log-plot for lag times $\tau = 0.1; 0.2; 0.4$ and 0.8 s. A similar linear relationship exists for $D_{\theta\theta}$, shown in Fig. 1 (b). The linear scaling of the correlation functions enables the estimation of η_s -independent quantities $\langle \mathbf{r} \cdot \mathbf{R}^{ij} \rangle_i$ and $\langle \mathbf{r} \cdot \mathbf{R}^{ij} \rangle_j$,

which depend only on R , and have units of a diffusion coefficient.

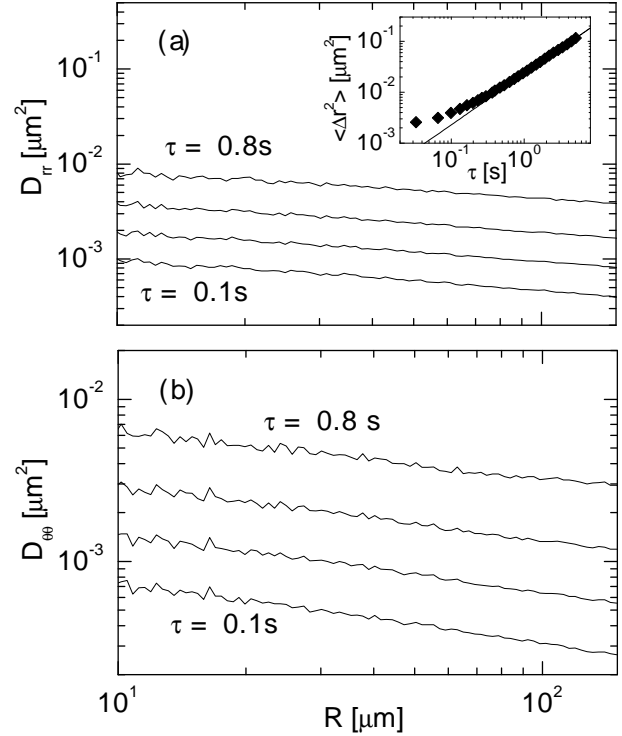


FIG. 1: (a) and (b) Two-point correlation functions $D_{rr}(R; \tau)$ and $D_{\theta\theta}(R; \tau)$ for a sample with $\eta_{s,1p} = 340$ nPa s m, with lag times $\tau = 0.1; 0.2; 0.4$ and 0.8 s. The evenly spaced correlation functions imply that $D_{rr}; D_{\theta\theta} \propto R^{-1}$. Inset: One-particle MSD for the sample (diamonds), where the straight line is a fit giving $\eta_{s,1p} = 340$ nPa s m, using Eqn. 2.

Changing the surface shear viscosity η_s , has a substantial effect on both D_{rr} and $D_{\theta\theta}$. At high η_s , Fig. 2 (a), both $\langle \mathbf{r} \cdot \mathbf{R}^{ij} \rangle_i$ and $\langle \mathbf{r} \cdot \mathbf{R}^{ij} \rangle_j$ are nearly equal and constant over the length scales $10 < R < 150$ μ m. At these surface viscosities, the behavior can be considered to be 2-D dominated, where the bulk fluid reservoirs have minimal influence. As η_s is decreased, Fig. 2 (b), we see curvature in these functions and deviation between their values, over the same range of length scales. At very low η_s , Fig. 2 (c), this deviation is even more pronounced, with $\langle \mathbf{r} \cdot \mathbf{R}^{ij} \rangle_i \propto R^{-1}$ and $\langle \mathbf{r} \cdot \mathbf{R}^{ij} \rangle_j \propto R^{-2}$. At these viscosities, bulk fluid effects begin to dominate, although the behavior is still 2-D as the protein molecules are confined to an interface. For all surface viscosities, the behavior of the correlation functions is markedly different from what is seen in bulk 3-D systems (where $D_{rr}; D_{\theta\theta} \propto R^{-1}$), and is sensitively dependent on η_s .

Despite the differences in the behavior of $\langle \mathbf{r} \cdot \mathbf{R}^{ij} \rangle_i$ and $\langle \mathbf{r} \cdot \mathbf{R}^{ij} \rangle_j$ at low and high surface viscosities, all the data can be scaled onto a single master curve. We define dimensionless correlation functions $\tilde{D}_{rr}; \tilde{D}_{\theta\theta} = D_{rr}; D_{\theta\theta} / \langle \mathbf{r} \cdot \mathbf{R}^{ij} \rangle_i$ and a reduced separation $\tilde{R} = R/L$,

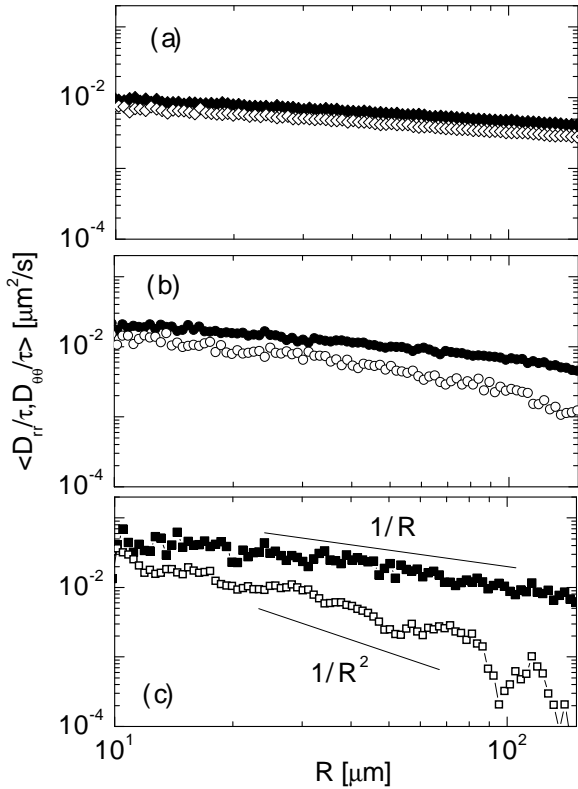


FIG. 2: Correlation functions $\langle D_{rr} \rangle$ (solid symbols) and $\langle D_{\theta\theta} \rangle$ (open symbols) as a function of particle separation R , for decreasing surface viscosities η_s . The samples are a) 2-D dominated: $\eta_{s,1p} = 340$ nPa s m (diamonds), b) Crossover: $\eta_{s,1p} = 72$ nPa s m (circles), c) 3-D dependent: $\eta_{s,1p} = 213$ nPa s m (squares).

where $L = \lambda_s = \lambda_s^0$. Both scale factors L and D_s depend only on η_s ; however, we allow them to vary independently to obtain two independent measures of η_s (η_s^0 and η_s^{av} respectively, in other words, $\lambda_s = R = \lambda_s^0$, and $D_s = k_B T = 4 \eta_s^{\text{av}}$). Fig. 3 shows the scaled variables D_{rr} , $D_{\theta\theta}$ plotted against the scaled separation $\beta = R \eta / \eta_s^0$. All the data sets fall on a single master curve, that spans nearly 4 orders of magnitude. This master curve has the characteristics of the individual data sets, at small β ($\beta \ll 1$), the curves are nearly logarithmic, at intermediate β ($\beta \sim 1$), they show crossover behavior, while at large β ($\beta \gg 1$), they show behavior that asymptotically approaches $1/R$ and $1/R^2$ for D_{rr} and $D_{\theta\theta}$ respectively. The solid lines are fits obtained from theoretical calculations of the response of an interface to a point force [10, 15], and have the form

$$D_{rr} = \left[-H_1(\beta) - \frac{2}{\beta} \left(Y_0(\beta) + Y_2(\beta) \right) \right]$$

$$D_{\theta\theta} = \left[H_0(\beta) - H_1(\beta) + \frac{2}{\beta} \left(Y_0(\beta) - Y_2(\beta) \right) \right] \beta$$

where the H are Struve functions, and the Y are Bessel

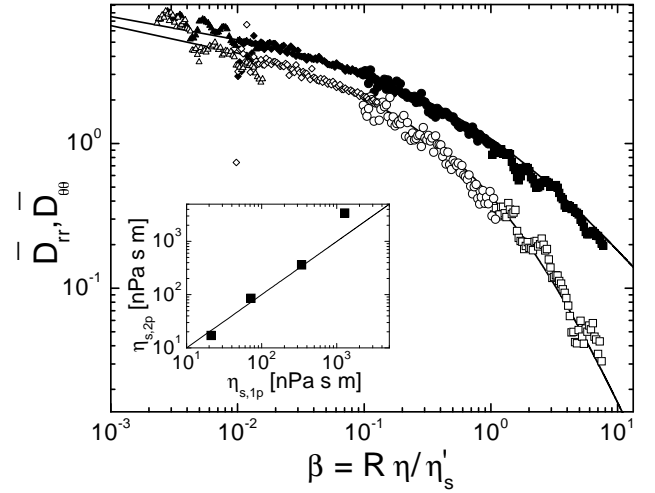


FIG. 3: Master curve of scaled variables D_{rr} (solid symbols) and $D_{\theta\theta}$ (open symbols) as a function of reduced particle separation β . Symbols are same as in Fig. 2, with an additional data set ($\eta_{s,1p} = 1275$ nPa s m; triangles). Solid lines represent theoretical fits to the data. Inset: One- and two-particle surface viscosities for the four samples shown in the master curve. The straight line has a slope of 1, indicating an equality between the two viscosities.

functions of the second kind. More importantly, up to a scale factor, Eqn. 3, and therefore the master curve, also characterizes the spatial dependence of the flow field at an interface in response to a perturbation, such as them alignment of tracers. To our knowledge, this is the first experimental mapping of this flow field over such a wide range of length scales.

The inset to Fig. 3 describes the scale factors used to create the master curve. For all the samples, the two independent estimates of the two-particle viscosity, $\eta_{s,2p}^0$ and $\eta_{s,2p}^{\text{av}}$, are within 15% of each other; we therefore plot their average, $\eta_{s,2p}$, against the one-particle viscosity $\eta_{s,1p}$. For most of the samples, the one- and two-particle measurements agree reasonably well with each other. However, at the highest viscosity, and therefore, the highest surface concentration of HSA, the two measurements deviate well beyond our experimental error. We believe this is a consequence of heterogeneity in the system; one possibility could be the formation of condensed phases at the interface at such high surface concentrations of HSA. While this would explain the underestimation of the true surface viscosity by the one-particle measurement, such an assumption deserves further study.

Conventional microrheology uses the one-particle MSD, $\langle \Delta r^2(t) \rangle$, to determine $G^0(\omega)$ and $G^{\text{av}}(\omega)$ [3]; these quantities are directly compared to bulk rheological measurements. Since the one-particle measurements are inherently local in nature, a more accurate approach is to determine the two-particle MSD [13], $\langle \Delta r^2(t) \rangle_{2p}$. Analogous to [13], we calculate this quantity for our 2-D viscous systems by extrapolating the long wavelength actual-

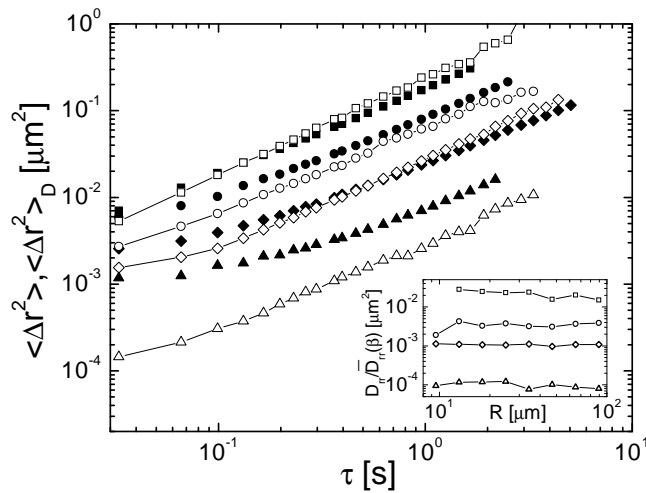


FIG. 4: One-particle (solid symbols) and two-particle (open symbols) MSDs for the samples shown in Fig. 3. Inset: radial scaling of D_{rr} for the different samples at a lag time $\tau = 0.53$ s.

tions of the medium to the bead size, which from Eqns. 2 and 3 gives

$$h r^2(\tau)_{1D} = 2h \frac{D_{rr}(R; \tau)}{D_{rr}(\tau)} i_R [\ln(2s/a) - E] \quad (4)$$

This expression can readily be generalized for viscoelastic interfaces, i.e., with a non-zero $G^0(\omega)$; however, such measurements are beyond the scope of this study. In practice, we confirm that $D_{rr}(R; \tau) = D(\tau)$ is nearly constant over the length scales studied, $9 < R < 100$ μ m,

shown in the inset to Fig. 4 for a specific lag time ($\tau = 0.53$ s). The averaged quantity $\langle D_{rr}(R; \tau) \rangle = D(\tau) i_R$ is then calculated for all lag times to obtain $h r^2(\tau)_{1D}$. From Fig. 4, we see that for all the samples, $h r^2(\tau)_{1D}$ is purely diffusive, as expected for a viscous system. At short lag times, the turnover in the one-particle MSDs, caused by resolution-limited noise, is significantly reduced in the two-particle MSDs. Finally, at long lag times, $h r^2(\tau)_{1D}$ is equal to $h r^2(\tau)$ within experimental error, except for the highest viscosity. These observations provide conclusive evidence of the accuracy of two-particle measurements over local probes of the rheology.

The verification of two-point microrheological techniques for a quasi-2D systems has applications for the study of inhomogeneous materials at an interface. Any significant variation between $h r^2(\tau)_{1D}$ and $h r^2(\tau)$ indicates the presence of heterogeneities, and the estimation of rheological quantities from the motion of tracer particles can be modified to reflect this. Future work will involve studying lipid molecules at an interface under compression/expansion, which creates domains such as liquid expanded or liquid condensed phases. We expect that our two-particle measurements will provide accurate measurements of the surface viscosity even with the presence of these heterogeneities. Other possible areas of future research are biological interfaces such as cell membranes, with the diffusing entities being protein aggregates or lipid rafts.

We thank G. C. Ianni, P. N. Segre and Alex J. Levine for helpful discussions. V. Prasad and Eric R. Weeks gratefully acknowledge support from NASA (Grant No. NAG 3-2728).

-
- [1] A. Einstein, Ann. Phys. 17, 549 (1905).
 [2] W. Sutherland, Phils. Mag. 9, 781 (1905).
 [3] T. G. Mason and D. A. Weitz, Phys. Rev. Lett. 74, 1250 (1995).
 [4] B. R. Dasgupta and D. A. Weitz, Phys. Rev. E. 71 (2005), 021504.
 [5] M. L. Gardel, M. T. Valentine, J. C. Crocker, A. R. Bausch, and D. A. Weitz, Phys. Rev. Lett. 91 (2003), 158302.
 [6] C. Y. Xu, V. Breedveld, and J. Kopecek, Biomacromolecules 6, 1739 (2005).
 [7] M. Sickert and F. Rondelez, Phys. Rev. Lett. 90 (2003), 126104.
 [8] A. Palle, P. Keller, E. L. Florin, K. Simons, and J. K. H. Horber, J. Cell Bio 148, 997 (2000).
 [9] Y. Gambin, R. Lopez-Esparza, M. Reay, E. Sierecki, N. S. Gov, M. Genest, R. S. Hodges, and W. Urbach, Proc. Natl. Acad. Sci. USA 103, 2098 (2006).
 [10] H. A. Stone and A. Ajdari, J. Fluid. Mech. 369, 151 (1998).
 [11] T. M. Fischer, J. Fluid. Mech. 498, 123 (2004).
 [12] P. G. Saman and M. Delbruck, Proc. Natl. Acad. Sci. USA 72, 3111 (1975).
 [13] J. C. Crocker, M. T. Valentine, E. R. Weeks, T. Gisler, P. D. Kaplan, A. G. Yodanis, and D. A. Weitz, Phys. Rev. Lett. 85, 888 (2000).
 [14] A. J. Levine and T. C. Lubensky, Phys. Rev. Lett. 85, 1774 (2000).
 [15] A. J. Levine and F. C. MacKintosh, Phys. Rev. E. 66 (2002), part 1 061606.
 [16] J. R. Lu, T. J. Su, and J. Penfold, Langmuir 15, 6975 (1999).
 [17] P. Chen, S. Lahooti, Z. Policova, M. A. Cabrerizo-Vilchez, and A. W. Neumann, Colloids And Surfaces B-Bio interfaces 6, 279 (1996).